



Innovative Approaches for the Sedimentological Characterization of Fine Natural and Anthropogenic Sediments in Karst Systems: The Case of the Apuan Alps (Central Italy)

Alessia Nannoni^{1*}, Leonardo Piccini¹, Pilario Costagliola¹, Nicolò Batistoni¹, Pietro Gabellini¹, Raffaello Cioni¹, Gabriele Pratesi² and Silvia Bucci²

¹ Department of Earth Science, Università degli Studi di Firenze, Florence, Italy, ² Agenzia Regionale per la Protezione Ambientale della Toscana, Florence, Italy

OPEN ACCESS

Edited by:

Davide Tiranti,
 Agenzia Regionale per la Protezione
 Ambientale (ARPA), Italy

Reviewed by:

Nadja Zupan Hajna,
 Research Centre of the Slovenian
 Academy of Sciences and Arts,
 Slovenia
 William White,
 Pennsylvania State University (PSU),
 United States

*Correspondence:

Alessia Nannoni
 alessia.nannoni@unifi.it

Specialty section:

This article was submitted to
 Quaternary Science, Geomorphology
 and Paleoenvironment,
 a section of the journal
 Frontiers in Earth Science

Received: 26 February 2021

Accepted: 08 April 2021

Published: 29 April 2021

Citation:

Nannoni A, Piccini L,
 Costagliola P, Batistoni N, Gabellini P,
 Cioni R, Pratesi G and Bucci S (2021)
 Innovative Approaches
 for the Sedimentological
 Characterization of Fine Natural
 and Anthropogenic Sediments
 in Karst Systems: The Case of the
 Apuan Alps (Central Italy).
 Front. Earth Sci. 9:672962.
 doi: 10.3389/feart.2021.672962

The Apuan Alps (NW Tuscany) is an important area of Central Italy characterized by large karst systems mainly fed via direct and diffuse water infiltration (autogenic recharge). These waters usually transport a clastic sediment load, originated by natural, surface and subsurface rock erosion/weathering which, in part, is deposited underground. In the Apuan Alps, during extreme rain event, huge amounts of carbonate powder, produced as a waste resulting from the quarrying operations of the famous “Carrara” marble, mix up with meteoric waters forming a slurry that is transported through the karst openings into the caves, where the carbonate powder may be deposited along with natural sediments. Depending upon karst hydrology and water fluxes, the slurry may eventually reach karst springs heavily reducing water quality. Mineralogical composition of the sediments collected along karst waterways and springs shows variable proportions of calcite associated with dolomite and silicates particles whereas the marble powder samples from quarry areas are mainly composed by calcite grains. Cave deposits of natural origin have usually a fine-sand grain size whereas spring sediments have a more variable grain-size distribution. Marble powder mainly has a silt grain size and produces a sort of “granulometric and morphometric pollution” which influences the transport mechanism of solid load through the karst systems along both vadose and phreatic waterways.

Keywords: karst, cave deposits, groundwater, solid load, Apuan Alps

INTRODUCTION

Caves represent one of the most relevant depositional archives in continental areas. This depends on the possibility that sediments can be preserved for very long times without undergoing significant weathering processes (Sasowsky, 2007). Among the typical cave deposits, those due to carbonate precipitation (speleothems) are by far the most studied because of the possibility to obtain paleoclimatic and paleoenvironmental data with very high temporal resolution (e.g., Fairchild and Baker, 2012 and references there in). Ancient clastic deposits, despite being volumetrically the most

common deposits in caves, are much less studied due to the difficulties of dating (Häuselmann et al., 2020) and of determining their source areas. Recently, an increasing interest has been focused to these deposits because their deposition is strongly related to landscape erosion phases and to extreme flood events, which are correlated with the local climate evolution (Karkanas and Goldberg, 2013). Moreover, transport and depositional dynamics of these sediments have important implications in archeology and paleontology (Martini, 2011).

Cave clastic sediments are usually divided into two categories: allogenic and autogenic sediments (White, 2007). Deposits related to allogenic supply through sinking streams are frequent in both active and relict karst systems (Springer, 2019). The sedimentological investigation of allogenic deposits allows also to get insights on the hydrological functioning of karst aquifers (Bosch and White, 2007; Bella et al., 2020). Autogenic deposits, derived from material coming from the karst system itself, are less common because the weathering processes affecting karst areas are mainly of chemical nature (dissolution) and therefore they do not virtually produce clastic sediments. The autogenic cave deposits are often derived from fragments produced by rock collapses that directly affect the path of the active passages. In this case, the clastic component has variable dimensions and irregular shapes, and a roundness depending on the greater or lesser transport it has undergone. Deposits of this type are generally found only in sectors affected by a consistent high energy flow. Fine carbonate deposits, usually ranging from fine sands to silt grain-size, are also found in caves (e.g., Zupan Hajna, 2002; Zupan Hajna et al., 2008). In this case, carbonate clasts are considered the product of subterranean weathering processes of limestone and dolomite (Zupan Hajna, 2003). Fine autogenic sediments usually occur in the epiphreatic and phreatic portions of karst systems, where they are transported in water-filled conduits. In these conditions transport involves only medium and fine-grained materials (sands, silt, clays) that can run through the entire system up to water outlets (karst springs). Hence, the textural features of these sediments are potentially able to provide us with information on the dynamics and therefore on the structure of the phreatic zones of karst systems (e.g., Winkler et al., 2016). Available literature is mainly focused on the physical and hydraulic properties of these sediments as suspended load during storm events but contributions on the systematic mineralogical, morphological and sedimentological characterization of these deposits are scarce (Drysdale et al., 2001; Herman et al., 2007; Piccini et al., 2019).

The Apuan Alps (AA), in north-western Tuscany, is a very peculiar mountain range in the Mediterranean basin, with many geological and biological features of international interest. This mountain area, whose maximum elevation is 1942 m asl at Pisanino Mount, consists of both metamorphic and non-metamorphic carbonate rocks belonging to three different tectonic units (Carmignani and Kligfield, 1990). The Apuan metamorphic unit is mainly represented by phyllites of the Paleozoic basement (Conti et al., 1993), meta-dolostones, marbles and dolomitic marbles (about 115 km² as outcrops) and by cherty limestones (about 20 km²) (Figure 1). Carbonate formations (meta-dolostones and marbles) host well-developed

karst landforms and several caves, including some of the largest and deepest of Italy (Piccini, 1998). Karstification developed since late Pliocene following the progressive exhumation of the carbonate sequences. Some major stages of karst development are related to tectonics and paleo-hydrological readjustment of river network (Piccini, 1998; Piccini et al., 2003), whereas climate changes are mainly recorded by cave chemical deposits (e.g., Isola et al., 2019). In the AA, the karst systems frequently host autogenic sediments. They are mainly composed by calcite and dolomite with minor amounts of silicates, thus reflecting the local origin of these sediments, the active role of the natural weathering processes as well as the significant solid load transport effectiveness of the phreatic sectors of karst aquifer.

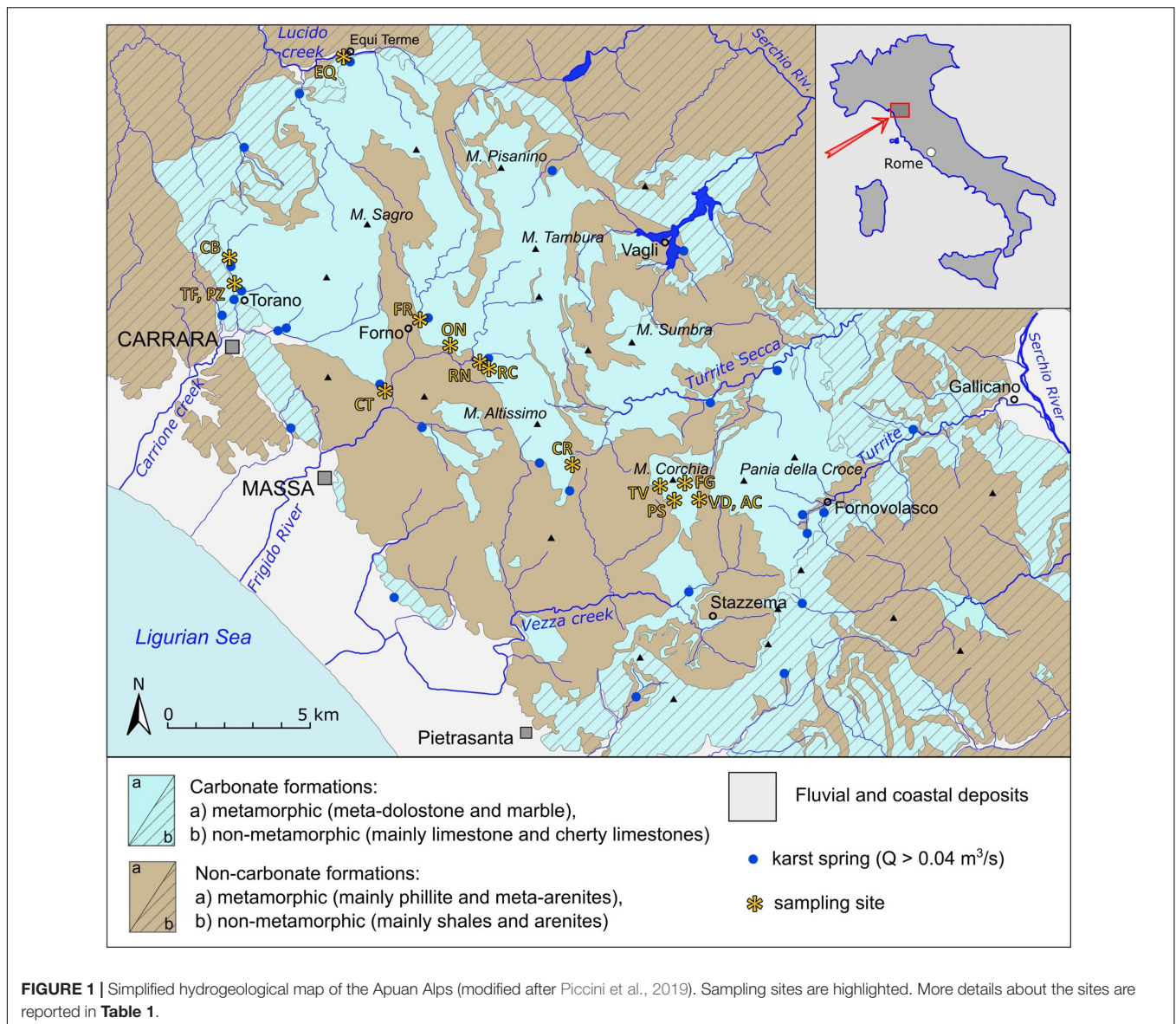
In the AA, variable amounts of carbonate powder, resulting from the quarrying operations of the worldwide famous “Carrara” marble, are mixed up with meteoric waters during storm events, forming a slurry that is rapidly transported throughout the karst openings into caves (Ekmekci, 1990; Rizzo et al., 2008). There it may be deposited along with natural sediments, modifying their composition. A significant portion of the slurry may reach the numerous springs fed by AA karst systems (Doveri et al., 2019). Consequently, springs may be temporarily affected by huge solid transport phenomena that determine a high turbidity during the flood events (Drysdale et al., 2001; Piccini et al., 2019).

The aim of this pilot study, which uses also unconventional methods and approaches, is to characterize the mineralogical, sedimentological, and morphological features of cave and spring sediments collected in some of the major AA karst systems. The same approach was applied to a few samples of marble powders produced by block sawing in the AA quarrying district. Cave and spring sediments were then compared to the quarry marble powder to investigate how anthropogenic materials can affect clastic sedimentation processes in presently active cave and karst spring environments.

MATERIALS AND METHODS

Twelve sampling sites (Figure 1) were selected to study the mineralogical, grain size, and morphological characteristics of cave deposits and to infer their source area and transport dynamic. Two main types of sampling environments were chosen: (1) some of the major AA karst springs, (2) some vadose cave passages, both active and inactive ones. Furthermore, samples were collected also in some quarries, where the marble powder is produced, as examples of the endmember of anthropogenic origin (Figure 2).

About 1 dm³ of sediment was collected in a LDPE bag at each site using a Teflon spoon, reducing the use of metallic tools to avoid contamination. The samples were dried at 45°C, then they were passed through a 2.8 mm sieve to remove impurities such as vegetal material and coarse particles accidentally occurring in the samples. The fraction passing through a 0.250 mm sieve was used for XRD, SEM-EDS and Optical Morphometric (OM) analyses. The sieved fraction to be analyzed was divided one or several



times in a sample splitter to obtain small but well-representative quantities (up to a few tens of grams).

Samples Description

The sampled deposits have been grouped as follows (**Table 1**): (1) cave sediments deposited in active vadose passages (active cave sediments), (2) cave sediments deposited in relict vadose passages (relict cave sediments), (3) cave-spring and karst spring deposits transported in phreatic flow condition (spring sediments), and (4) marble powder produced by different sawing techniques (diamond wire and chain sawing). Most of the active and relict cave sediments were collected in the Corchia cave system, one of the largest and complex caves in Italy (Piccini et al., 2008; Piccini, 2011). Relict deposits were also collected in the Buca dell'Onice, an inactive cave in the Frigido River basin containing a thick clastic deposit (Piccini et al., 2003). In the same river basin, active

cave deposits were collected into the Buca del Rocciolo e Buca di Renara, two caves that are occasionally inundated during major floods. Three sediment samples were collected in the Buca di Equi, in northern AA, a cave-spring which is partially inundated during floods. Other sediments come from Vauclausian-type springs fed by submerged and inaccessible conduits. Samples that were transported in phreatic conditions and were collected in caves close to the outlet (referred as “cave-spring” in the text) are considered as karst spring deposits.

Analytical Methods

The analyses were performed only on the fraction passing through a sieve with a diameter of 0.250 mm ($\varphi > 2$, i.e., from fine sands to clay grain size) to optimize the adopted instrumental micro-procedures that require a small quantity of sediment (1–3 mm³). Anyway, almost systematically, the sediment fraction

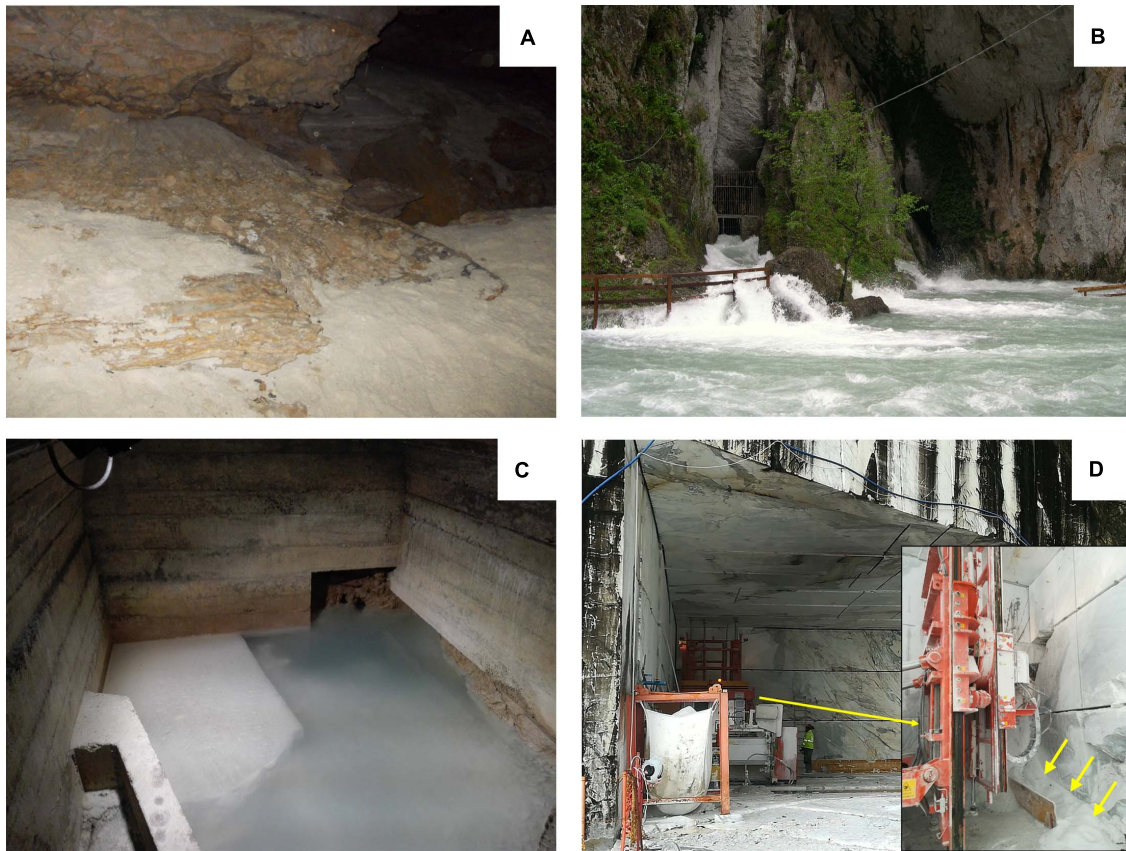


FIGURE 2 | Examples of the chosen sampling sites: **(A)** fine clastic deposit in an occasionally active vadose passage of the Antro del Corchia cave; **(B)** cave-spring outlet (see the text for the terminology) of Buca d'Equi cave during a flood; **(C)** fine whitish deposits in the Tana dei Tufi water gallery, a spring strongly affected by marble slurry pollution; **(D)** quarrying sector where marble powder is produced (yellow arrows point to the powder).

with a diameter exceeding this threshold was negligible (less than 10% of the total volume). Furthermore, the fine components are the most relevant sediment fraction for this study, since they are more easily transported as suspended solid in flowing water and therefore can travel long distances also in phreatic conditions.

XRD measurements were performed at the Centro di Servizi di Cristallografia Strutturale (CRIST) of the Florence University with a Bruker Da Vinci D8 diffractometer operating with a Cu X-ray source, a Theta-Theta goniometer, and a flat Eulero Cradle sample holder, equipped with a Bruker LYNXEYE-XE detector. The filament current of the tube was 40 mA and the acceleration potential 40 kV. Yttrium oxide (Y_2O_3) was used as a reference material.

Samples for microchemical analyses were prepared by means of the sample dispersion unit (SDU) of the image particle analyzer (see below for description): the sediment particles were scattered over a stub (diameter = 12.5 mm) covered with an adhesive graphite tape. This method allowed to properly separate sediment particles and to homogeneously distribute them on the stub. Finally, the samples were carbon-sputtered with a Quorum Q150R ES sample metallizer. Microchemical compositions of the samples were investigated by means of a Scanning Electron Microscope (ZEISS EVO MA15, operating at 15 kV acceleration

voltage), coupled with an Energy Dispersive Spectrometer (OXFORD INCA 250 EDS detector and software INCA Feature, Oxford Instruments®) at the Centro di Microscopia Elettronica e Microanalisi (MEMA) of the Florence University. Images were collected using both Secondary Electrons (SE) and Backscattered Electron (BSE) imaging. The software setup was fixed to analyze at least 2000–3500 particles with a circle equivalent diameter larger than 0.0038 mm. Based on EDS micro-chemical analyses, grains were classified in four categories during post processing: calcite, dolomite, silicate, and unclassified particles.

Particles having Ca > 5 wt% (weight percentage) were classified as carbonate grains, then a Ca/Mg ratio of 2 (expressed in moles) was selected as threshold between calcite and dolomite. This value was chosen because of the short acquisition time (4 s) for each particle micro-analysis that often results in a systematic underestimate of the Mg content. Grains that presented Si > 2 wt% were identified as silicate minerals. The particles that did not fall in these three mineral groups were considered “unclassified” and not considered in the dataset analysis. The unclassified group comprises (a) organic matter and metallization residuum (maximum 15% of the analyzed grains), and (b) accessory minerals such as sulfates, oxides/hydroxides, apatite (maximum 2.5% of the analyzed grains).

TABLE 1 | List of the collected samples (the letters of the sample code refer to the sampling site reported in **Figure 1**).

Code	Type	Sampling site	Description
ON.01	Cave, relict	Buca dell'Onice cave, Frigido basin	Terminal chamber, upper deposit
ON.02	Cave, relict	Buca dell'Onice cave, Frigido basin	Terminal chamber, lower deposit
RC.02	Cave, relict	Buca del Rocciolo cave, Frigido basin	Relict epiphreatic passage
FG.01	Cave, relict	Figliera, Corchia cave, Vezza basin	Relict vadose passage
FG.02	Cave, relict	Figliera, Corchia cave, Vezza basin	Relict vadose passage
FG.03	Cave, relict	Figliera, Corchia cave, Vezza basin	Relict vadose passage
AC.01	Cave, relict	Antro del Corchia cave, Vezza basin	Relict vadose passage
VD.05	Cave, relict	Antro del Corchia cave, Vezza basin	Relict vadose passage
VD.01	Cave, active	Antro del Corchia cave, Vezza basin	Active vadose passages
VD.02	Cave, active	Antro del Corchia cave, Vezza basin	Active vadose passages
VD.03	Cave, active	Antro del Corchia cave, Vezza basin	Occasionally inundated chamber
VD.04	Cave, active	Antro del Corchia cave, Vezza basin	Occasionally inundated chamber
VD.06	Cave, active	Antro del Corchia cave, Vezza basin	Active vadose passages
RC.01	Cave, active	Buca del Rocciolo cave, Frigido basin	Epiphreatic passage
CT.01	Karst spring	Cartaro spring, Frigido basin	Spring, settling pool
FR.01	Karst spring	Forno spring, Frigido basin	Spring deposit
FR.02	Karst spring	Forno spring, Frigido basin	Spring deposit
RN.01	Karst spring	Renara spring, Frigido basin	Cave-spring, settled suspended sediment
EQ.01	Karst spring	Buca d'Equi cave, Lucido basin	Cave-spring, close to the cave outlet
EQ.02	Karst spring	Buca d'Equi cave, Lucido basin	Cave-spring, upper passage
EQ.03	Karst spring	Buca d'Equi cave, Lucido basin	Cave-spring, settled suspended sediment
TF.01-t	Karst spring	Tana dei Tufi aqueduct, Carrione basin	Top part of a deposit in an open channel
TF.01-b	Karst spring	Tana dei Tufi aqueduct, Carrione basin	Lower part of a deposit in an open channel
CB.01	Karst spring	Carbonera spring, Carrione basin	Access gallery to the aqueduct
PZ.01	Karst spring	Pizzutello spring, Carrione basin	Main aqueduct, below water surface
CR.01	Quarry	Cervaiole quarry, Altissimo mount	Marble powder, wet chain sawing
CR.02	Quarry	Cervaiole quarry, Altissimo mount	Marble powder, diamond wire
TV.01	Quarry	Tavolini B quarry, Corchia mount	Marble powder, wet chain sawing

(Continued)

TABLE 1 | Continued

Code	Type	Sampling site	Description
TV.02	Quarry	Tavolini B quarry, Corchia mount	Marble powder, diamond wire
PS.03	Quarry	Piastraio quarry, Corchia mount	Marble powder, diamond wire
PS.04	Quarry	Piastraio quarry, Corchia mount	Marble powder, wet chain sawing
PS.05	Quarry	Piastraio quarry, Corchia mount	Marble powder, dry chain sawing

Morphometric and grain-size analyses (MGS) were performed with an automated optical analyzer for particle characterization (Morphologi G3, Malvern InstrumentsTM). The instrument measures basic parameters (length, width, perimeter, and area) of each particle with diameter ranging from 0.0015 mm up to 3 mm. The software calculates several shape parameters such as circle equivalent diameter (CED), aspect ratio (AR), circularity (C), solidity (S), and convexity (Cv). CED is defined as the diameter of a circle with the same area of the particle 2D-projection. AR, C, S, and Cv are non-dimensional shape parameters defined, respectively, as: the width over the length of the particle, the circle equivalent perimeter over the real particle perimeter, the particle projected area over the particle convex hull area, and the particle convex hull perimeter over the particle perimeter. More details about the instrument and operating protocols can be found in Leibrandt and Le Pennec (2015). The morphometric analysis is presented only for particles falling in the fine to coarse silt size interval (0.0625 – 0.0078 mm, $\phi = 4 - 7$). This specific grain size interval was selected because it comprises a considerable proportion of particles for all the samples in terms of both volume and number of grains, and because the analysis in narrow size intervals is more helpful for revealing characteristics for these kinds of material (Leibrandt and Le Pennec, 2015; Li et al., 2019). Grain size distributions (GSD) were calculated in volume fractions (V%) and in number of particles (n%) falling in CED intervals of $1/2 \phi$ (Folk and Ward, 1957; Blott and Pye, 2012). We stress that GSD expressed as number of particles is not a standard sedimentological method, but it is a reliable approach when dealing with grain size data obtained with optical methods instead of sieving, because it allows to distinguish better the grain size differences in the finer portions of sediments (González-Tello et al., 2010).

RESULTS

Grains Mineralogy and Micro-Morphology

XRD analyses showed that the sediments collected in caves and karst springs are mainly composed by calcite, dolomite and secondarily by silicates (**Figure 3**). Calcite and dolomite greatly vary in their relative quantities, as estimated by their diagnostic XRD peak intensities. As expected, quarry samples are made up of calcite only, being marble almost pure metamorphosed limestone (Cantisani et al., 2005).

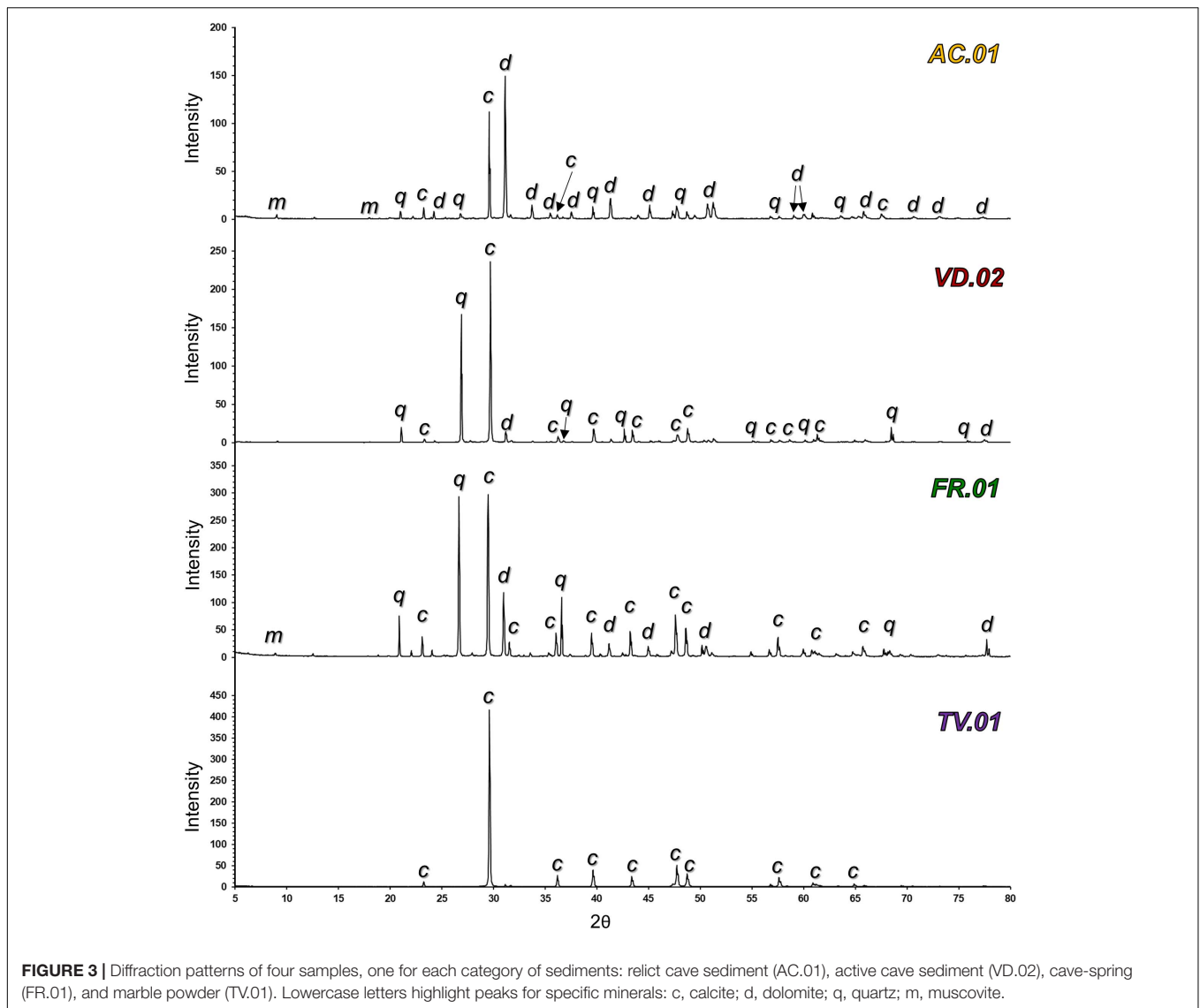
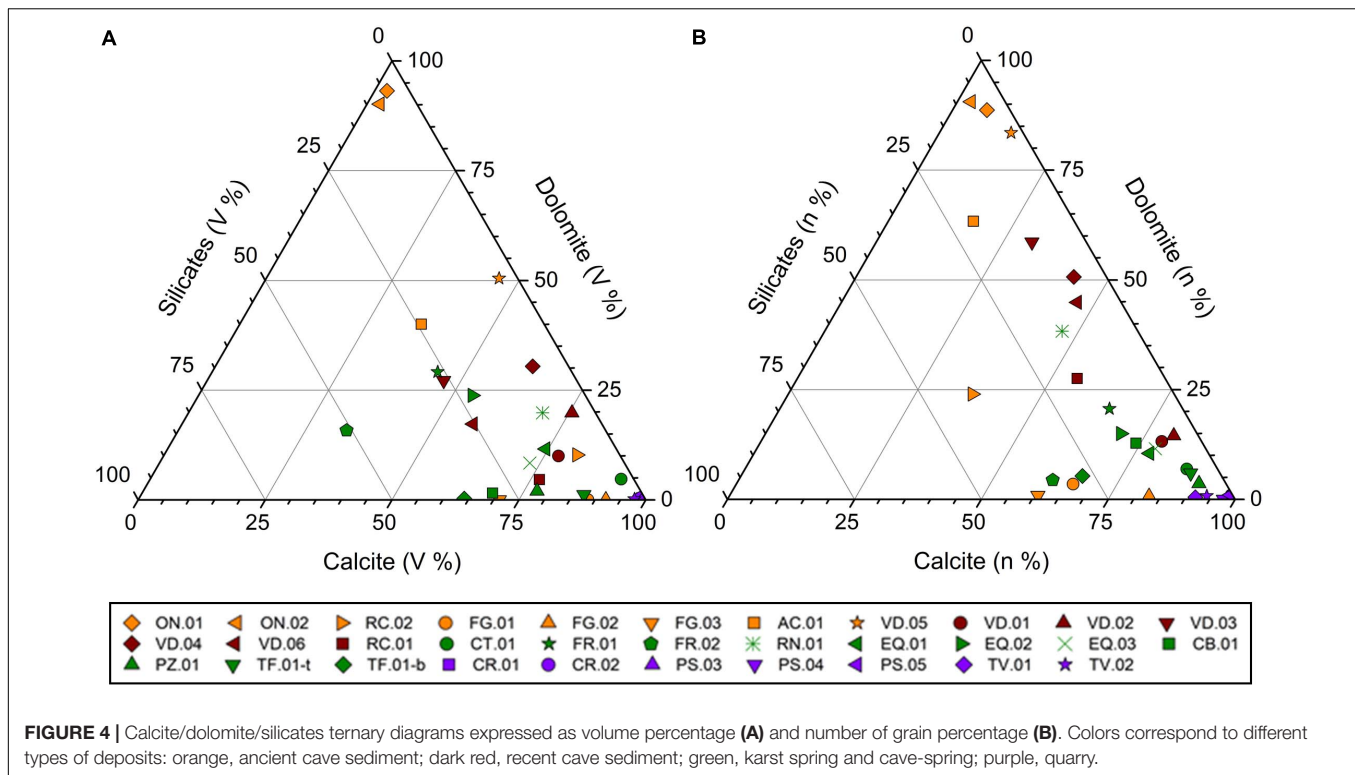


FIGURE 3 | Diffraction patterns of four samples, one for each category of sediments: relict cave sediment (AC.01), active cave sediment (VD.02), cave-spring (FR.01), and marble powder (TV.01). Lowercase letters highlight peaks for specific minerals: c, calcite; d, dolomite; q, quartz; m, muscovite.

SEM-EDS analyses made it possible: to quantify the abundances of the main constituents (calcite, dolomite, and silicates), to observe the shape of the particles, and to get some insights on the grain size of each constituent. Silicate minerals occur with variable proportions in all the studied categories of deposits, but never exceed 50%. The compositional features of the samples are shown in the two ternary diagrams of **Figure 4**. The figure illustrates how the relative proportions of the three main mineralogical constituents can drastically change for many samples if the volume (**Figure 4A**; V%) or the number of particles (**Figure 4B**; n%) is considered. This effect is due to the inhomogeneous size distribution of the three minerals. In the V% diagram, the mineral proportions are indeed heavily influenced by the composition of the coarse fraction, whereas the nature of fine grains determines the position of the samples in the n% diagram, because they are numerically much more abundant than the coarser particles, although volumetrically irrelevant. Ideally, the sample points remaining

in the same position in the two diagrams are those having a similar GSD of the three main mineralogical components. Therefore, the grain size of dolomite, quartz and calcite may be highlighted by the relative positions occupied by a sample in the two diagrams.

Samples having a uniform composition, such as quarry materials (CR.01, CR.02, PS.03, PS.04, PS.05, TV.01, and TV.02) and the two cave deposits consisting almost exclusively of dolomite (ON.01 and ON.02) maintain the same location in the two diagrams. Conversely, samples having a variable composition can greatly change their position. For example, sample FR.02 is placed more on the right in the V% diagram respect to the n% diagram, indicating that the silicate and dolomite particles are coarser than the calcite grains. In general, we observe that spring samples have usually more variable proportions of silicates and dolomite but are dominated by fine calcite grains and tend to move toward the calcite corner in the n% diagram. Conversely, most of the cave deposits tend to move toward the dolomite



vertex, indicating that dolomite particles usually have a finer grain size than calcite ones.

Particles also show distinctive features of the surface. Some carbonate particles show clear traces of dissolution (Figures 5A,B), possibly due to natural weathering processes. The surfaces of the clasts of natural origin are always irregular and engraved by small cavities caused by etching such as V-in-V micro-morphologies (Figure 5A) frequently observed in calcite and dolomite exposed to chemical aggressive environments (Viles and Moses, 1998). On the contrary, the particles produced by the cutting and squaring of the marble blocks are usually more euhedral with no evidence of dissolution (Figures 5C,D). Spring and active cave samples exhibit both micro-morphologies (Figures 5E,F). Where present, quartz grains usually show conchoidal fracture surfaces (Figure 5E).

Grain Size

Grain size analyses were obtained by means of the optical morphograinizer because this instrument allows a more statistically robust dataset based on a much greater number of particles respect to SEM-EDS. In the analyzed sediments, GDS obtained by means of SEM-EDS were found to not be reliable even considering the silt-size grains, in contrast to previous findings (Cheetham et al., 2008). The particle size analysis performed on the medium-fine portion (from 0.25 to 0.0015 mm) of the cave, cave-spring sediments and of the cutting-powder collected in quarries, showed quite variable characteristics (Figure 6).

Although only the $\varphi > 2$ fraction was analyzed, the GSD expressed as volume percent show substantial differences

between the sediment categories. Cave and spring sediments show a high variability of frequency in the $\varphi = 2.0$ – 2.5 and $\varphi = 2.5$ – 3.0 grain-size classes, even when considering samples collected in the same site (i.e., FR.01 and FR.02, Figure 6C), with values ranging from a few percent to 53%. This larger dispersion in the coarser fraction is possibly influenced by the poor representativeness for some of the analyzed samples for what concerns the coarser particles, due to the small quantity of material used for MGS analysis (1 – 3 mm^3). The graphs expressed in volume (Figures 6A,C,E) are therefore surely significant for all samples when $\varphi > 3$ ($\text{CED} > 0.125 \text{ mm}$) and mainly in the silt fraction ($\varphi = 4$ – 8). In this portion of the cave sediments graph (Figure 6A) we can distinguish two samples of relict sediments (ON.01 and ON.02) from all the others. The spring sediments show instead more uniform characteristics, although with significant differences in the classes between $\varphi = 3.5$ and $\varphi = 4.5$. The quarry materials, on the other hand, show two distinct groups based on grain size that reflect the origin of the powders whether produced by cutting with diamond wire (finer size, modal class $\varphi = 4.0$ – 4.5) or chain saws (coarser size, modal class $\varphi \leq 3.5$ – 4.0).

To overcome the representativeness problems linked to the representation in volume percentage and to emphasize the difference in the finer portion, GSD is plotted also as percentage in number of particles (Figures 6B,D,F). GSD expressed as number of particles is quite uniform in quarry powder. Cave sediments show relevant differences in the finer portion ($\varphi > 8$) where active cave deposits are usually finer than the relict cave ones. Spring sediments are also quite differentiated in the finer portion ($\varphi > 7$): CT.01, PZ.01, and FR.02 samples

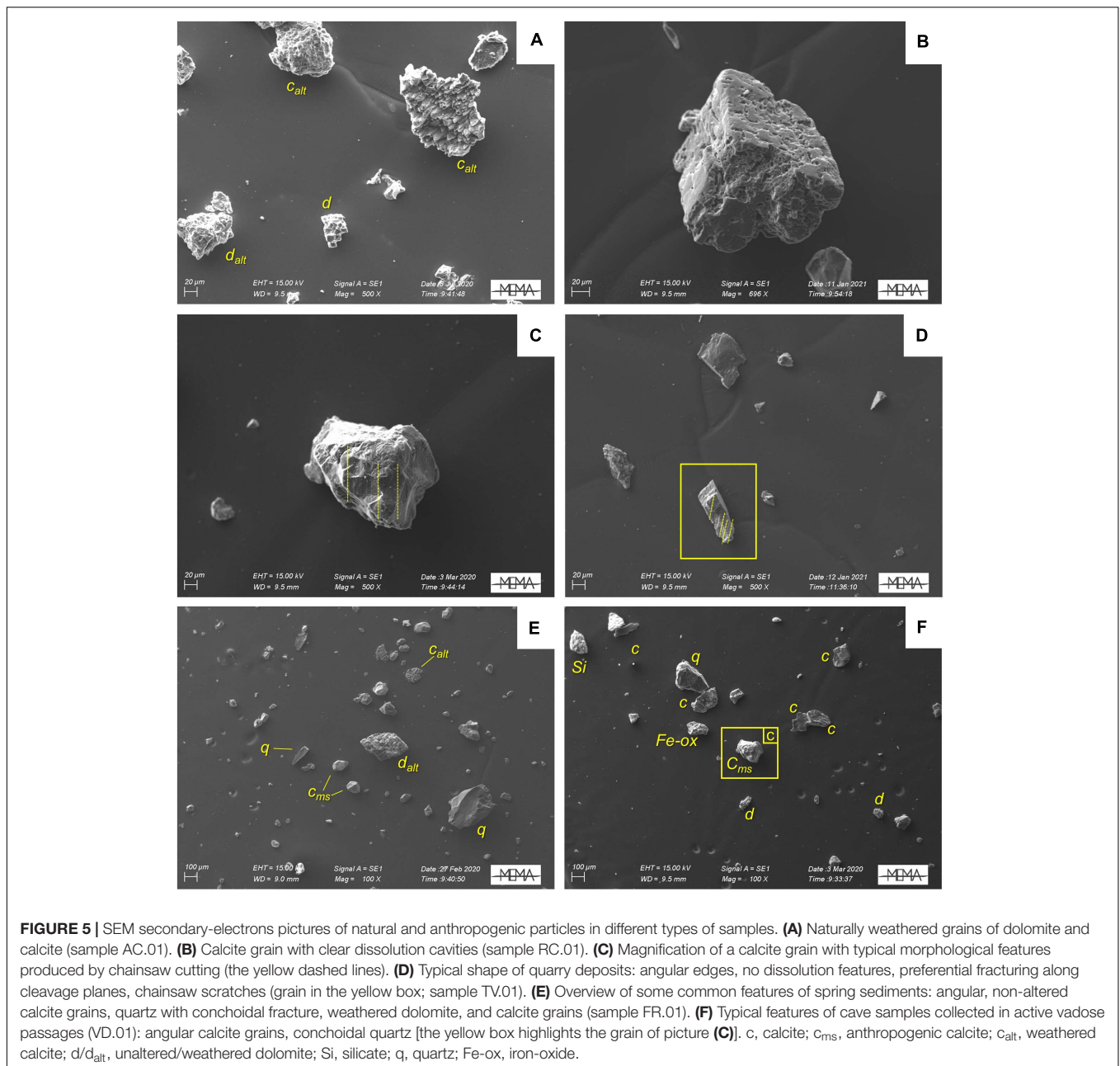


FIGURE 5 | SEM secondary-electrons pictures of natural and anthropogenic particles in different types of samples. **(A)** Naturally weathered grains of dolomite and calcite (sample AC.01). **(B)** Calcite grain with clear dissolution cavities (sample RC.01). **(C)** Magnification of a calcite grain with typical morphological features produced by chainsaw cutting (the yellow dashed lines). **(D)** Typical shape of quarry deposits: angular edges, no dissolution features, preferential fracturing along cleavage planes, chainsaw scratches (grain in the yellow box; sample TV.01). **(E)** Overview of some common features of spring sediments: angular, non-altered calcite grains, quartz with conchoidal fracture, weathered dolomite, and calcite grains (sample FR.01). **(F)** Typical features of cave samples collected in active vadose passages (VD.01): angular calcite grains, conchoidal quartz [the yellow box highlights the grain of picture **(C)**]. c, calcite; C_{ms} , anthropogenic calcite; C_{alt} , weathered calcite; d/d_{alt} , unaltered/weathered dolomite; Si, silicate; q, quartz; Fe-ox, iron-oxide.

have a modal class ($\varphi = 7.5\text{--}8$) coarser than the other samples ($\varphi \geq 8.5$).

Grain Morphometry

Analysis performed with the MGS provide also morphometrical data describing the shape (namely the shape of the projected particles outline) of each grain. The selected shape parameters (aspect ratio, circularity, convexity, and solidity) range, for all the types of samples, over a quite large interval of values, however, suggesting some important differences. Considering only the fine to coarse silt fraction, the mean values of the four selected shape parameters for the relict cave samples are comprised in the following ranges: AR = 0.64–0.75; C = 0.84–0.92; Cv = 0.97–0.99

and S = 0.94–0.98 (**Figure 7**). Their mean values for the active cave samples vary in the intervals: 0.66–0.74 for AR, 0.85–0.91 for C, 0.97–0.99 for Cv, and 0.95–0.98 for S. Karst spring samples have mean values of 0.68–0.70 for AR, 0.86–0.91 for C, 0.97–0.99 for Cv, and 0.94–0.98 for S. In the quarry samples, AR mean values range between 0.66 and 0.69, C mean values are comprised between 0.83 and 0.91, Cv is comprised in the 0.96–0.99 interval, and S mean values range between 0.93 and 0.98. Interquartile ranges are always asymmetrically distributed around the median value, with a large number of outliers that is generally smaller for the samples of marble powder. Interquartile ranges for AR are broader than those exhibited by the other parameters in all samples. Quarry samples display a slightly more dispersed

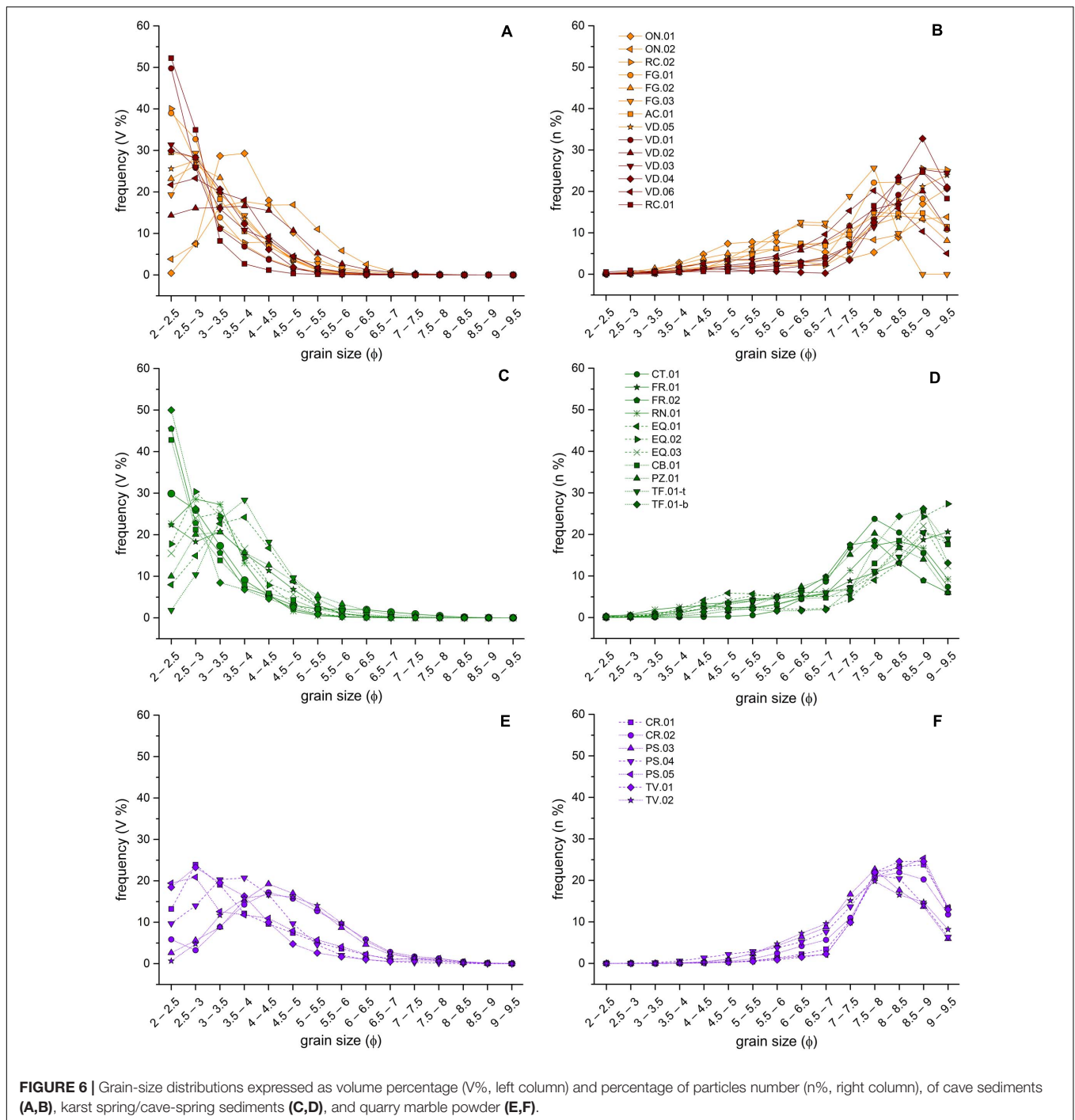


FIGURE 6 | Grain-size distributions expressed as volume percentage (V%, left column) and percentage of particles number (n%, right column), of cave sediments (A,B), karst spring/cave-spring sediments (C,D), and quarry marble powder (E,F).

distribution of C, S, and C_v than the other types of samples, whereas AR has its higher dispersion in the cave samples.

DISCUSSION

The different types of fine clastic sediments presented in this study have textural, morphological, sedimentological, and mineralogical characteristics that depend on several factors:

source area, transport mechanism, hydrodynamic conditions in the aquifer, deposition mechanisms, interplay between weathering and mechanical alteration, and, finally, supply from quarry powder. Consequently, it appears quite difficult to discriminate the role of each factor.

The abundance of carbonate sands and silt demonstrates the provenance of most of the clasts from the karst systems themselves and that the alteration processes of carbonate rocks produce solid material as well as solution load. A possible source

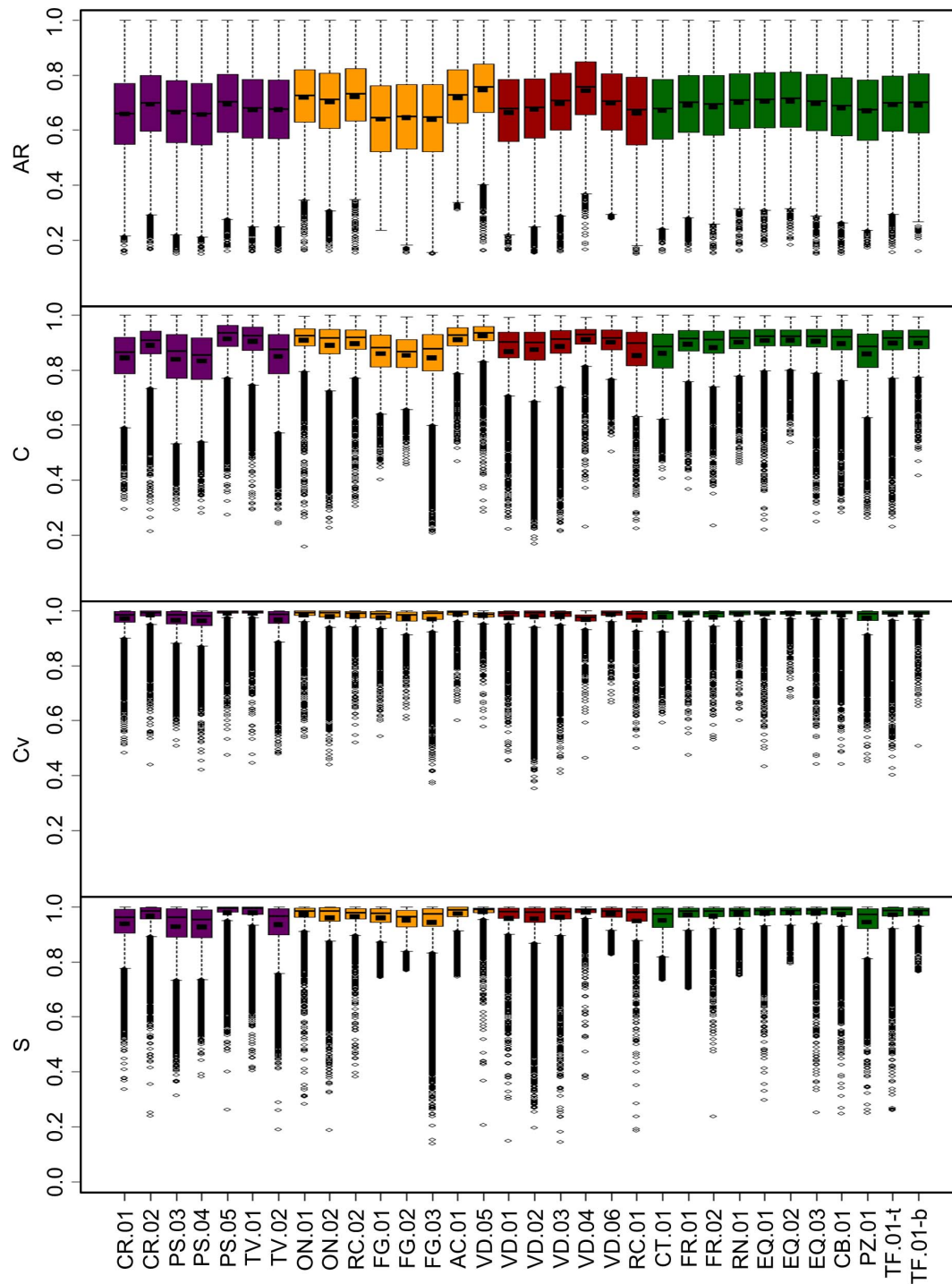
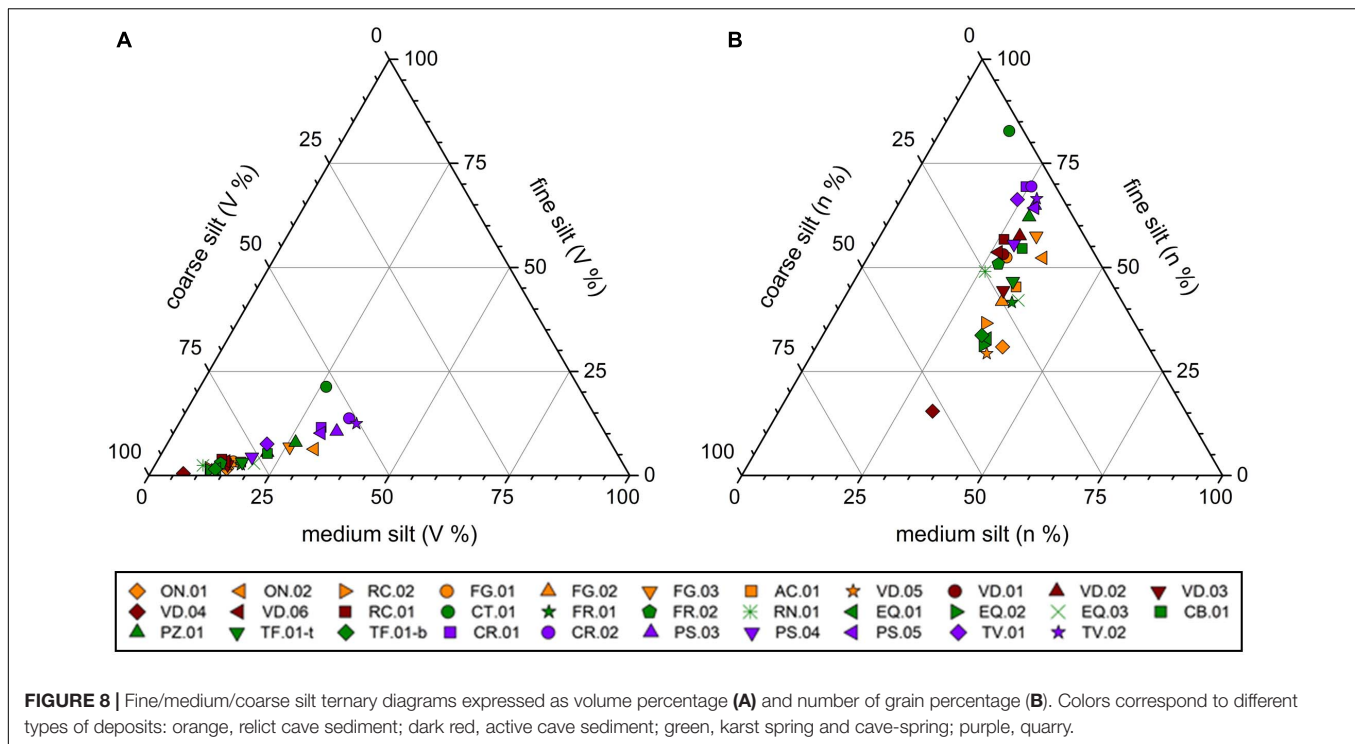


FIGURE 7 | Box-plots of aspect ratio (AR), circularity (C), convexity (Cv), and solidity (S) of the four types of samples in the fine to coarse silt size interval. Colors correspond to different types of deposits: purple, marble powder; orange, relict cave sediments; dark red, active cave sediments; green, karst spring/cave-spring sediments. Mean and median values and outliers are represented by in-box horizontal rectangles, solid segments and open circles, respectively.

of this autogenic clastic material is the incomplete dissolution of the carbonate rocks on cave walls due to chemically aggressive laminar flow and/or condensation water (Zupan Hajna, 2002, 2003). This is a selective process because it does not attack

frontally the rock, but it dissolves first the contacts between grains, microstructures and crystal imperfections, weakening the mechanical cohesion of the rock, and leaving powdery, weathered surfaces. The weathered wall rock can be mechanically eroded,

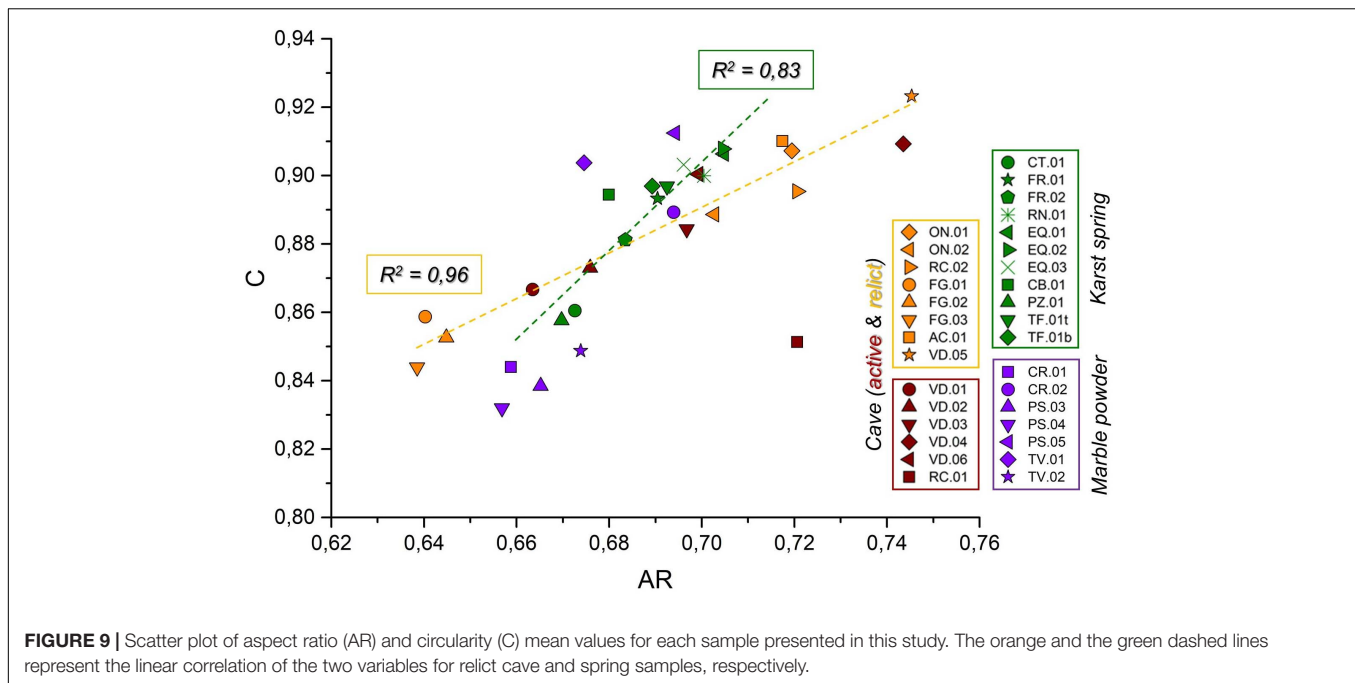


then the resulting carbonate particles can be transported through the karst network. In the AA, the occurrence of calcite grains in presently active cave and spring deposits could be mainly attributed to the contamination by the marble powders produced by the quarrying activities, which are widespread over almost the entire territory (see **Figure 1**). On the other hand, the sediment samples collected in no longer active sectors in the Corchia and Onice caves show that calcite clasts of natural origin can also be present. Dolomitic and silicate grains are instead surely due to natural weathering processes, as the lithologies that contain significant fractions of these components are not subject to excavation. The compositions of relict caves sediments vary from mostly calcitic to mostly dolomitic, demonstrating that both marbles and dolostones are subject to partial dissolution phenomena, which probably occur in the covered or semi-covered epikarst, where percolating waters have a greater dissolving power and can act for longer times. The lack of dissolution markers on the particles of anthropogenic origin, on the other hand, demonstrates that the waters that flow in the karst systems, both in vadose and phreatic conditions, have a low dissolving power, as there is no reason to think that the particles of natural origin have a longer residence time in the aquifer than those of anthropogenic origin.

In general, the silt fraction ($\varphi = 4-8$, i.e., from 0.0625 to 0.0039 mm) results as the most discriminant grain size fraction between the different sediment categories, when considering the portion finer than fine sand, probably because it depends more on the clast provenance (weathering of the host rock or anthropogenic sources) and it is more sensitive to the transport/deposition dynamic selection than the finer fraction, which is easily transported as suspended load. For all these

reasons, we investigated in detail the silt portion of sediments comparing as relative percentages the three following fractions: 0.0625 to 0.0312 mm (coarse silt), 0.0312 to 0.0156 mm (medium silt), and 0.0156 to 0.0078 mm (fine silt). Very fine silt (0.0078–0.0039 mm) was excluded from diagrams because it is more subject to be transported away as suspended load and hardly deposited either in cave or karst spring environments (Herman et al., 2012).

The ternary diagram with the three considered silt fractions expressed as volume percentage (**Figure 8A**) reveals an alignment of the samples along a trend that goes from the coarse silt vertex toward a mean composition consisting of about 50% coarse silt, 35% medium silt, and 15% fine silt, which corresponds to the powder produced by diamond wire cutting. The active cave sediments are found exclusively close to the coarse silt vertex, whereas quarry samples are on the other extreme of the trend, confirming their finer composition. Relict cave and spring sediments are more distributed along the trend but are generally coarser than the quarry samples. A less defined trend is observed also in the silt ternary diagram with the proportions expressed as percentage of particles number (**Figure 8B**). In this latter case all the sediments are distributed from 50% of coarse silt to 75–80% of fine silt. Moreover, the quarry samples are clustered over the finest fraction. The CT.01 spring sample stands out in both diagrams and it appears to be finer than the quarry samples produced by the diamond sawing. This spring was recognized to be heavily affected by marble slurry inputs that result in episodes of strong turbidity increases (Drysdale et al., 2001). Furthermore, this sample, unlike the others, comes from the decantation tank of the capture settlement and it is therefore probable that also the finest part of the sediment could have been deposited here, while



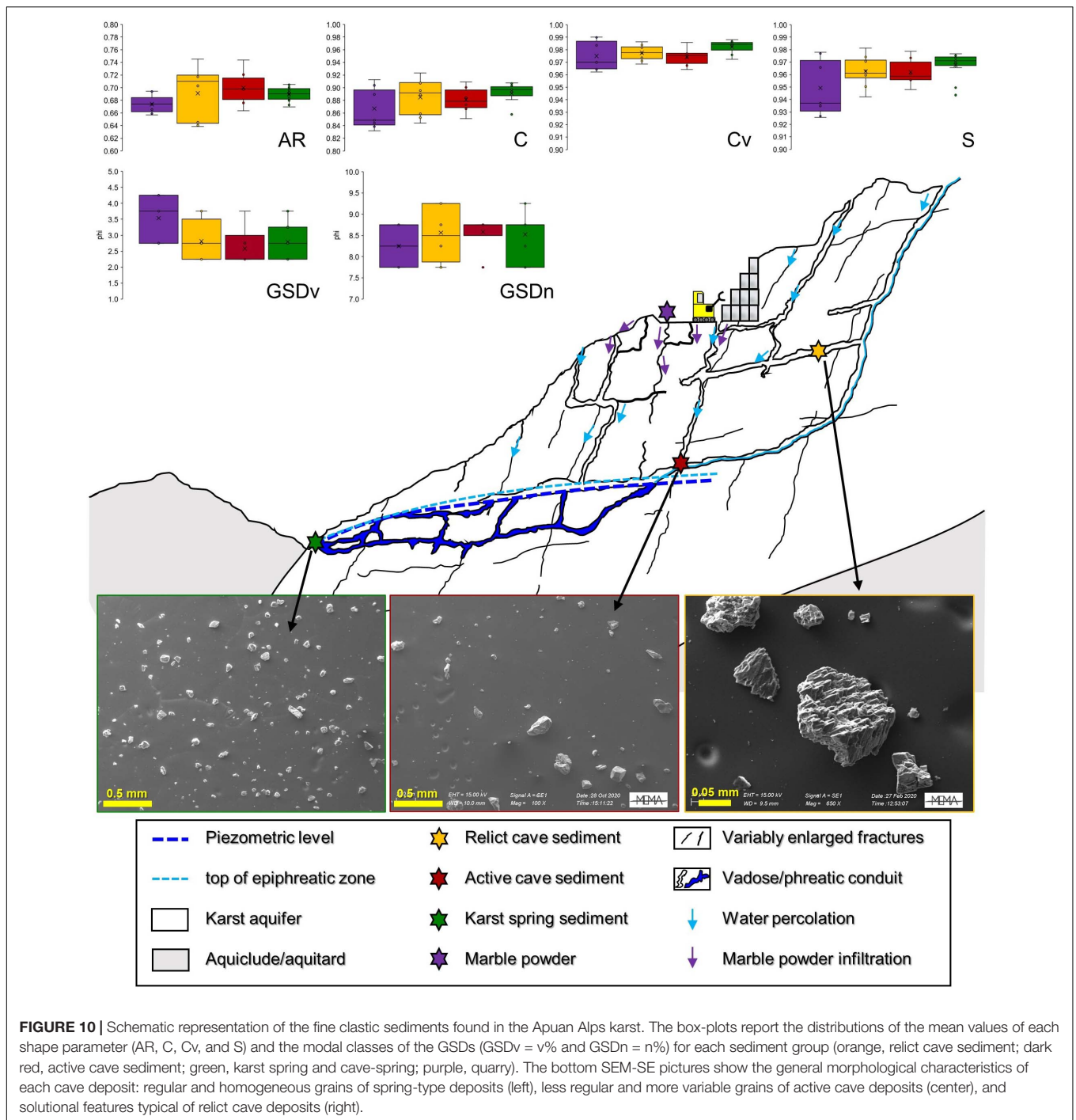
coarse silt may have been partially deposited during the transport through the aquifer in phreatic conditions.

Cave sediments have a higher percentage of coarse silt, probably because they have experienced transport in vadose conditions only, and the finer materials cannot be normally deposited in such conditions. Spring sediments, which have undergone also transport in phreatic conditions, are more distributed according to the different transport/deposition conditions they have experienced and to the structure of the phreatic zone of each system. In general, the samples collected in the spring with a greater flow rate (FR and EQ samples) have a higher percentage of coarse silt, while those of the smaller springs have a higher percentage of medium and fine silt. In some cases (CT.01, PZ.01, CB.01) the greater presence of medium/fine silt is certainly due to the occurrence of variable quantities of marble slurry coming from the quarries, also recognized during micro-morphological observations with SEM.

Morphometric comparison based on MSG analysis revealed some peculiar characteristics among sediments of different types: generally, cave samples show a greater variability in the distributions of shape parameters than those of spring samples. This is evident especially looking at aspect ratio and circularity distributions and secondarily at solidity (see **Figure 7**). This variability is probably due to the different deposition conditions that can occur in vadose streamways, which are characterized by a succession of pools, steps, and tight channels, where the flow velocity varies greatly. The very high number of outliers for the different shape parameters of sediments could reflect the heterogeneous composition of the natural sediments, although dominated by carbonate clasts. On the other hand, Cv and S of quarry samples have a larger interquartile range respect to those of natural sediments, suggesting more complex morphologies possibly related to the absence of a transport-related shape

modifications. Plotting the mean values of the aspect ratio against the mean circularity for each sample in a scatter diagram, a rough linear relationship occurs (**Figure 9**). This is partially expected because more elongated particles (lower AR) are usually far from having a regular shape (higher values of circularity). However, it is noteworthy to observe that two trends can be distinguished, one for relict cave sediments and one for spring samples. Active cave samples fall midway between these two trends whereas quarry samples are distributed around the spring samples trend. This means that, increasing AR, the circularity increases a little faster in spring samples and quarry material respect to relict cave sediments. This could be due to the occurrence in relict cave sediments of altered clasts with a less regular perimeter. Rough surfaces should determine a particle perimeter longer than that of the particle equivalent circle, resulting in lower values of circularity. Naturally weathered calcite and dolomite particles show in fact micro-morphologies (e.g., V-V shapes) that could increase the difference between the real particle perimeter and its equivalent circle, whereas spring samples and marble powder particles have angular but more regular surfaces, reducing the difference between the two perimeters. On the contrary, AR is not sensitive to the roughness of the perimeter. In other words, it is possible that these two trends are related to the different flow conditions that spring and cave sediments experienced, and, regarding the marble powder, to its different origin. The morphological similarities between the spring and the marble powder samples could be also partially related to the fact that the quarry material can infiltrate into the karst systems and ultimately reach the karst springs, mixing with natural sediment particles.

Figure 10 summarizes the position within a karst system of the types of samples collected and their characteristics (presented with box-plots of the mean values for each parameter). The comparison of the different sediment types permits to make some



general assessments about the transport and deposition dynamics in the AA karst systems, although the ranges of variability for the sedimentological, morphological, and mineralogical features of the deposits somewhat overlap. Overall, it can be said that the AA karst systems are not particularly granulometric-selective, at least when dealing with materials in the dimensional range investigated in this study. This observation is probably related to the overall flow organization in the AA karst systems: these aquifers are characterized by well-developed vadose and

epiphreatic flow systems that determine fast and impulsive responses to precipitation, with extremely variable flowrates (Doveri et al., 2019). Phreatic flow is concentrated in a few enlarged conduits that are probably able to transport silt to fine sands sediments without significant size selection. Marble powder exhibits the finest GSD (v%) but once it infiltrates in the aquifers, its size is only partially discriminant between natural and anthropogenic-contaminated sediments. This could mean that (a) its finest fraction is washed away so it cannot be found

in the karst system, and (b) its medium to coarse fraction (i.e., the silt) variably mixes with a natural sediment that is fine itself so the marble input does not cause a significant shift in the grain size, except for the springs more heavily polluted. The morphological variability of the sediments collected in the vadose zone is strongly dependent on the choice of the sampling site: the deposition in vadose conditions is extremely site-specific due local variations of flow conditions. Therefore, samples collected only a few meters apart can exhibit different characteristics. On the other hand, sediments collected at the karst springs show the most regular morphologies probably because flow in the phreatic zone determines a morphometric selection (Baba and Komar, 1981; Garzanti et al., 2008), permitting to the most regular, but not necessarily the most rounded, particles to reach the karst system outlet. Phreatic conduits have an adverse (upward) conduit gradient in the streamwise direction that produces saturated flow conditions. Consequently, there is a fluid energy threshold for sediment transport in this portion of the karst systems. This threshold controls the sediment storage in the aquifer and it is in turn dependent on the phreatic zone architecture (Husic et al., 2017). Thus, particle settling is favored between upward sections of phreatic conduits and grains with rough and irregular surfaces are hardly re-mobilized after they settle because roughness increases both the angle of repose and the viscous friction for rolling particles (Beakawi Al-Hashemi and Baghabra Al-Amoudi, 2018). These phenomena are less relevant for regular grains so that they can be transported more efficiently to the karst springs. Marble powder shows the highest variability and the lowest values in the shape factors (except for AR) because of its origin: the shape of the particles is generally angular, but it could also depend on the direction of sawing respect to the orientations of anisotropic features (cleavage) occurring in the rock massif.

CONCLUSION

The analyzed cave and spring sediments are mainly composed of calcite, dolomite and silicates in ratios that primarily depend on the nature of the rocks outcropping in the respective feeding basins and on the presence of materials coming from the quarries. The occurrence of a significant percentages of dolomite indicates that the carbonate rocks are subject to a partial dissolution that releases the individual granules making them then subject to mechanical erosion. This process is probably favored in the AA by the saccharoidal (sugar-like) structure of the metamorphosed dolostones and limestones (Cantisani et al., 2009; Gulli et al., 2015).

Calcite grains due to weathering processes have a very different surface micromorphologies from those produced by the marble sawing. The former in fact show evident traces of dissolution, while the latter have flat faces that tend to follow the calcite cleavage. Therefore, this feature is useful for the qualitative distinction between natural and anthropogenic calcite grains.

The compositional and sedimentological analyzes of cave and spring deposits collected in some karst systems of the AA have shown quite heterogeneous characteristics in

each studied category. The anthropogenic component, coming from the extraction of marble, is present in very variable percentage in almost all recent sediments but it is difficult to be quantified because its mineralogical and morpho-dimensional features partly fall within the range of variability of the natural deposits. Furthermore, this implies a good transport capacity of the entire karst systems and therefore their low dimensional selective capacity. The hydrodynamic conditions in the phreatic zones may determine a morphometric selection, consequently the particles of spring deposits have more regular and homogenous shapes respect to vadose zone samples. These observations are crucial with regards to the arrangement of the phreatic zone of the AA karst systems: these aquifers are generally characterized by extensive vadose and epiphreatic flow systems, whereas phreatic flow occurs along few, highly conductive, karstic conduits. This arrangement could be responsible for the morphometric and granulometric features observed in the AA spring sediments: phreatic flow occurs with enough energy to prevent granulometric selection and good transport capacity (at least for fine materials). However, the relatively low flow velocities in the phreatic conduits limit preferentially the mobilization/re-mobilization and transport of irregular particles respect to the regular ones, accordingly to our results.

It is also evident that there is a high variability between samples collected in the same site, which depends on the local conditions in which the sedimentation occurs. This poses a sampling problem that introduces a possible bias in the characterization of the various types of deposits. On the other hand, the presence of marble powder from quarries, whose characteristics appear relatively distinctive, offers the possibility of using this material as a sort of tracer to characterize the various aquifer systems from a hydrodynamic point of view. For the continuation of the research, it is therefore necessary to associate the various sediments with the hydraulic characteristics of each groundwater systems, comparing the sedimentological investigations with the results of the hydrogeological monitoring of underground streams and karst springs.

DATA AVAILABILITY STATEMENT

The datasets presented in this article are not readily available because they will be used for other publications. Requests to access the datasets should be directed to the corresponding author.

AUTHOR CONTRIBUTIONS

AN: SEM-EDS and XRD analyses, data processing, figures drawing, and writing of the manuscript. LP: research coordination, data analysis, and writing of the manuscript. PC: research coordination, data interpretation, and manuscript revision. NB, PG, and RC: MSG analyses and data interpretation. GP: data analysis. SB: research coordination. All authors contributed to the scientific discussion of the data and agreed to the submitted version of the manuscript.

FUNDING

This research was funded by a grant of the Agenzia Regionale per la Protezione Ambientale della Toscana (ARPAT) in the framework of CAVE project (Framework agreement Rep. 381/2017).

REFERENCES

- Baba, J., and Komar, P. D. (1981). Measurements and analysis of setting velocities of natural quartz sand grains. *J. Sediment. Res.* 51, 631–640. doi: 10.2110/jsr.51.631
- Beakawi Al-Hashemi, H. M., and Baghabra Al-Amoudi, O. S. (2018). A review on the angle of repose of granular materials. *Powder Technol.* 330, 397–417. doi: 10.1016/j.powtec.2018.02.003
- Bella, P., Gradziński, M., Hercman, H., Leszczyński, S., and Nemeč, W. (2020). Sedimentary anatomy and hydrological record of relic fluvial deposits in a karst cave conduit. *Sedimentology* 68, 425–448. doi: 10.1111/sed.12785
- Blott, S. J., and Pye, K. (2012). Particle size scales and classification of sediment types based on particle size distributions: review and recommended procedures. *Sedimentology* 59, 2071–2096. doi: 10.1111/j.1365-3091.2012.01335.x
- Bosch, R. F., and White, W. B. (2007). “Lithofacies and transport of clastic sediments in karstic aquifers,” in *Studies of Cave Sediments*, eds I. D. Sasowsky and J. Mylroie (Dordrecht: Springer Netherlands), 1–22. doi: 10.1007/978-1-4020-5766-3_1
- Cantisani, E., Fratini, F., Malesani, P., and Molli, G. (2005). Mineralogical and petrophysical characterisation of white Apuan Marble. *Per. Mineral.* 74, 117–140.
- Cantisani, E., Pecchioni, E., Fratini, F., Garzonio, C. A., Malesani, P., and Molli, G. (2009). Thermal stress in the Apuan marbles: relationship between microstructure and petrophysical characteristics. *Int. J. Rock Mech. Mining Sci.* 46, 128–137. doi: 10.1016/j.ijrmmms.2008.06.005
- Carmignani, L., and Kligfield, R. (1990). Crustal extension in the northern Apennines: the transition from compression to extension in the Alpi Apuane Core Complex. *Tectonics* 9, 1275–1303. doi: 10.1029/tc009i006p01275
- Cheatham, M. D., Keene, A. F., Bush, R. T., Sullivan, L. A., and Erskine, W. D. (2008). A comparison of grain-size analysis methods for sand-dominated fluvial sediments. *Sedimentology* 55, 1905–1913. doi: 10.1111/j.1365-3091.2008.00972.x
- Conti, P., Di Pisa, A., Gattiglio, M., and Meccheri, M. (1993). “The pre-alpine basement in the Alpi Apuane (Northern Apennines, Italy),” in *Pre-Mesozoic Geology in the Alps*, eds F. Neubauer and J.F.v Raumer (Berlin: Springer), 609–621. doi: 10.1007/978-3-642-84640-3_36
- Doveri, M., Piccini, L., and Menichini, M. (2019). “Hydrodynamic and Geochemical features of metamorphic carbonate aquifers and implications for water management: the apuan Alps (NW Tuscany, Italy) case study,” in *The Handbook of Environmental Chemistry*, eds T. Younos, M. Schreiber, and C. Kosic Ficco (New York, NY: Springer International Publishing), 209–249. doi: 10.1007/978-3-319-77368-1_8
- Drysdale, R. N., Pierotti, L., Piccini, L., and Baldacci, F. (2001). Suspended sediments in karst spring waters near Massa (Tuscany), Italy. *Environ. Geol.* 40, 1037–1050. doi: 10.1007/s002540100311
- Ekmekci, M. (1990). “Impact of quarries on karst groundwater systems,” in *Hydrogeological Processes in Karst Terranes*, Vol. 207, eds G. Gunay, A. I. Johnson, and W. Back (Wallingford: IAHS), 3–6.
- Fairchild, I. J., and Baker, A. (2012). *Speleothem Science*. Hoboken, NJ: John Wiley & Sons, Ltd, doi: 10.1002/9781444361094
- Folk, R. L., and Ward, W. C. (1957). Brazos River bar [Texas]; a study in the significance of grain size parameters. *J. Sediment. Res.* 27, 3–26. doi: 10.1306/74d70646-2b21-11d7-8648000102c1865d
- Garzanti, E., Andò, S., and Vezzoli, G. (2008). Settling equivalence of detrital minerals and grain-size dependence of sediment composition. *Earth Planet. Sci. Lett.* 273, 138–151. doi: 10.1016/j.epsl.2008.06.020
- González-Tello, P., Camacho, F., Vicaria, J. M., and González, P. A. (2010). Analysis of the mean diameters and particle-size distribution in powders. *Part. Part. Syst. Charact.* 27, 158–164. doi: 10.1002/ppsc.200900097
- Gulli, D., Pellegri, M., and Marchetti, D. (2015). “Mechanical behavior of Carrara marble rock mass related to geo-structural conditions and in-situ stress,” in *Proceedings of the 15th Pan-American Conference on Soil Mechanics and Geotechnical Engineering (PCSMGE)/8th South American Congress on Rock Mechanics (SCRM)*, Buenos Aires, Argentina, 15–18 November 2015, eds A. O. Sfriso, D. Manzanal, and R. J. Rocca (Amsterdam: IOS Press), 253–260.
- Häuselmann, P., Plan, L., Pointner, P., and Fiebig, M. (2020). Cosmogenic nuclide dating of cave sediments in the Eastern Alps and implications for erosion rates. *IJS* 49, 107–118. doi: 10.5038/1827-806x.49.2.2303
- Herman, E. K., Tancredi, J. H., Toran, L., and White, W. B. (2007). Mineralogy of suspended sediment in three karst springs. *Hydrogeol. J.* 15, 255–266. doi: 10.1007/s10040-006-0108-2
- Herman, E. K., Toran, L., and White, W. B. (2012). Clastic sediment transport and storage in fluviokarst aquifers: an essential component of karst hydrogeology. *Carbonates Evaporites* 27, 211–241. doi: 10.1007/s13146-012-0112-7
- Husic, A., Fox, J., Agouridis, C., Currens, J., Ford, W., and Taylor, C. (2017). Sediment carbon fate in phreatic karst (Part 1): conceptual model development. *J. Hydrol.* 549, 179–193. doi: 10.1016/j.jhydrol.2017.03.052
- Isola, I., Ribolini, A., Zanchetta, G., Bini, M., Regattieri, E., Drysdale, R. N., et al. (2019). Speleothem U/Th age constraints for the Last Glacial conditions in the Apuan Alps, northwestern Italy. *Palaeogeogr. Palaeoclimatol. Palaeoecol.* 518, 62–71. doi: 10.1016/j.palaeo.2019.01.001
- Karkanas, P., and Goldberg, P. (2013). “6.23 micromorphology of cave sediments,” in *Treatise on Geomorphology*, eds J. Shroeder and A. Frumkin (Amsterdam: Elsevier), 286–297. doi: 10.1016/b978-0-12-374739-6.00120-2
- Leibrandt, S., and Le Pennec, J.-L. (2015). Towards fast and routine analyses of volcanic ash morphometry for eruption surveillance applications. *J. Volcanol. Geoth. Res.* 297, 11–27. doi: 10.1016/j.jvolgeores.2015.03.014
- Li, K. M., Zuo, L., Nardelli, V., Alves, T. M., and Lourenço, S. D. N. (2019). Morphometric signature of sediment particles reveals the source and emplacement mechanisms of submarine landslides. *Landslides* 16, 829–837. doi: 10.1007/s10346-018-01123-1
- Martini, I. (2011). Cave clastic sediments and implications for speleogenesis: new insights from the Mugnano Cave (*Montagnola Senese*, Northern Apennines, Italy). *Geomorphology* 134, 452–460. doi: 10.1016/j.geomorph.2011.07.024
- Piccini, L. (1998). Evolution of karst in the Apuan Alps (Italy): relationships with the morphotectonic history. *Suppl. Geografia Fisica e Dinamica Quaternaria* 3, 21–31.
- Piccini, L. (2011). Speleogenesis in highly geodynamic contexts: the quaternary evolution of Monte Corchia multi-level karst system (Alpi Apuane, Italy). *Geomorphology* 134, 49–61. doi: 10.1016/j.geomorph.2011.06.005
- Piccini, L., Di Lorenzo, T., Costagiola, P., and Galassi, D. M. P. (2019). Marble slurry’s impact on groundwater: the case study of the Apuan Alps Karst Aquifers. *Water* 11:2462. doi: 10.3390/w11122462
- Piccini, L., Drysdale, R., and Heijnis, H. (2003). Karst morphology and cave sediments as indicators of the uplift history in the Alpi Apuane (Tuscany, Italy). *Q. Int.* 10, 219–227. doi: 10.1016/s1040-6182(02)00104-0
- Piccini, L., Zanchetta, G., Drysdale, R. N., Hellstrom, J., Isola, I., Fallick, A. E., et al. (2008). The environmental features of the Monte Corchia cave system (Apuan Alps, central Italy) and their effects on speleothem growth. *IJS* 37, 153–172. doi: 10.5038/1827-806x.37.3.2
- Rizzo, G., D’Agostino, F., and Ercoli, L. (2008). Problems of soil and groundwater pollution in the disposal of “marble” slurries in NW Sicily. *Environ. Geol.* 55, 929–935. doi: 10.1007/s00254-007-1043-9
- Sasowsky, I. D. (2007). Clastic sediments in caves – imperfect recorders of processes in Karst. *Acta Carsol.* 36, 143–149. doi: 10.3986/ac.v36i1.216
- Springer, G. S. (2019). “Clastic sediments in caves,” in *Encyclopedia of Caves*, eds W. White, D. Culver, and T. Pipan (Amsterdam: Elsevier), 277–284. doi: 10.1016/b978-0-12-814124-3.00031-5
- Viles, H. A., and Moses, C. A. (1998). Experimental production of weathering nanomorphologies on carbonate stone. *Q. J. Eng. Geol. Hydrogeol.* 31, 347–357. doi: 10.1144/gsl.qjeg.1998.031.p4.08

ACKNOWLEDGMENTS

The authors would like to thank the editor and the two reviewers for their helpful comments that helped to improve the manuscript.

- White, W. B. (2007). Cave sediments and paleoclimate. *J. Cave Karst Stud.* 69, 76–93.
- Winkler, T. S., van Hengstum, P. J., Horgan, M. C., Donnelly, J. P., and Reibenspies, J. H. (2016). Detrital cave sediments record Late Quaternary hydrologic and climatic variability in northwestern Florida, USA. *Sedimentary Geol.* 335, 51–65. doi: 10.1016/j.sedgeo.2016.01.022
- Zupan Hajna, N. (2002). Origin of fine-grained carbonate clasts in cave sediments. *Acta Carsologica* 31, 115–137. doi: 10.3986/ac.v31i2.392
- Zupan Hajna, N. (2003). “Chemical weathering of limestone and dolomites in a cave environment,” in *Evolution of Karst: from Prekarst to Cessation*, ed. F. Gabrovsek (Ljubljana: ZRC), 347–356.
- Zupan Hajna, N., Pruner, P., Mihevc, A., Schnabl, P., and Bosák, P. (2008). Cave Sediments from Postojnska–Planinska cave system (Slovenia): evidence of multi-phase evolution in epiphreatic zone. *Acta Carsologica* 37, 63–86. doi: 10.3986/ac.v37i1.160
- Conflict of Interest:** The authors declare that the research was conducted in the absence of any commercial or financial relationships that could be construed as a potential conflict of interest.
- Copyright © 2021 Nannoni, Piccini, Costagliola, Batistoni, Gabellini, Cioni, Pratesi and Bucci. This is an open-access article distributed under the terms of the Creative Commons Attribution License (CC BY). The use, distribution or reproduction in other forums is permitted, provided the original author(s) and the copyright owner(s) are credited and that the original publication in this journal is cited, in accordance with accepted academic practice. No use, distribution or reproduction is permitted which does not comply with these terms.